Chinese Chemical Letters 35 (2024) 109660

Contents lists available at ScienceDirect

Chinese Chemical Letters

journal homepage: www.elsevier.com/locate/cclet

Development of a multi-level pH-responsive lipid nanoplatform for efficient co-delivery of siRNA and small-molecule drugs in tumor treatment

Yunjie Dang[a,1], Yanru Feng[a,b,1], Xiao Chen[a,1], Chaoxing He[a], Shujie Wei[a], Dingyang Liu[a], Jinlong Qi[c], Huaxing Zhang[c], Shaokun Yang[a,*], Zhiyun Niu[d,*], Bai Xiang[a,*]

[a] Department of Pharmaceutics, Hebei Medical University, Shijiazhuang 050017, China
[b] Department of Pharmacy, The Fourth Hospital of Hebei Medical University, Shijiazhuang 050011, China
[c] Core Facilities and Centers, Hebei Medical University, Shijiazhuang 050017, China
[d] Department of Hematology, The Second Hospital of Hebei Medical University, Shijiazhuang 050000, China

ARTICLE INFO

Article history:
Received 9 December 2023
Revised 8 February 2024
Accepted 15 February 2024
Available online 17 February 2024

Keywords:
Cyclic peptides
siRNA
Liposomal platform
Multi-level pH-responsive
Co-delivery

ABSTRACT

The combination of nucleic acid and small-molecule drugs in tumor treatment holds significant promise; however, the precise delivery and controlled release of drugs within the cytoplasm encounter substantial obstacles, impeding the advancement of formulations. To surmount the challenges associated with precise drug delivery and controlled release, we have developed a multi-level pH-responsive co-loaded drug lipid nanoplatform. This platform first employs cyclic cell-penetrating peptides to exert a multi-level pH response, thereby enhancing the uptake efficiency of tumor cells and endow the nanosystem with effective endosomal/lysosomal escape. Subsequently, small interferring RNA (siRNA) complexes are formed by compacting siRNA with stearic acid octahistidine, which is capable of responding to the lysosome-to-cytoplasm pH gradient and facilitate siRNA release. The siRNA complexes and docetaxel are simultaneously encapsulated into liposomes, thereby creating a lipid nanoplatform capable of co-delivering nucleic acid and small-molecule drugs. The efficacy of this platform has been validated through both *in vitro* and *in vivo* experiments, affirming its significant potential for practical applications in the co-delivery of nucleic acids and small-molecule drugs.

Tumors have long been recognized as a significant peril to human well-being and survival. Traditional gene interference therapy, specifically RNA interference (RNAi), has emerged as a highly promising approach for treating cancer and other ailments [1–4]. Nevertheless, the limited efficacy in delivering therapeutic agents [5], along with issues of instability [6] and suboptimal gene silencing efficiency, severely hinder the broader implementation of this therapy in clinical settings [7–10]. Additionally, the delivery of nucleic acid drugs to the cytoplasm and ensuring sustained effects pose further challenges in the treatment process [11,12]. The development of a targeted cytoplasmic effective and stable siRNA delivery system is of great significance for the precision diagnosis and treatment of major diseases such as tumors.

To improve the stability of the small interferring RNA (siRNA) delivery process, researchers mostly use positively charged substances to absorb the siRNA to form a complex [13,14], thereby safeguarding it against enzymatic degradation within the organism. However, the presence of numerous negatively charged substances in the organism can readily induce the off-target effect of siRNA. Consequently, lipid nanoplatforms can be utilized to encapsulate the compressed siRNA complex, thereby further improving its stability within the organism and alleviating the off-target effects of siRNA [15–17]. Moreover, the successful delivery of drugs to the lesion site is also hindered by notable physiological barriers, primarily due to the requirement for siRNA to operate within the cytoplasm. Prior to reaching the cytoplasm, siRNA is prone to capture by lysosomes, which house diverse enzymes capable of degrading siRNA. Even if evading the lysosomal capture, the release of siRNA encounters further impediments. Therefore, this project, based on previous laboratory studies [18], uses stearic acid and octa histidine to form the pH-responsive copolymer SA-H_8, which exhibits hydrophobicity under physiological conditions and can

* Corresponding authors.
E-mail addresses: yangshaokun@hebmu.edu.cn (S. Yang), zhiyunniu@hebmu.edu.cn (Z. Niu), baixiang@hebmu.edu.cn (B. Xiang).
[1] These authors contributed equally to this work.

https://doi.org/10.1016/j.cclet.2024.109660
1001-8417/

effectively compress water-soluble siRNA. Moreover, SA-H_8 can respond to changes in gradient pH. In late endosomes/lysosomes (pH 4.0–5.5), SA-H_8 assumes a more positively charged state, leading to a tighter binding with negatively charged siRNA molecules. This enhanced binding serves to safeguard the siRNA from enzymatic degradation. Upon SA-H_8/si escape from the endosomes/lysosomes and arrival in the cytoplasm (pH 7.4), SA-H_8 once again responds to pH fluctuations. Specifically, the imidazole group on its histidine undergoes deprotonation, resulting in the neutralization of SA-H_8. Consequently, the electrostatic interaction between SA-H_8 and siRNA is disrupted, facilitating the successful release of siRNA. This strategy effectively addresses the challenges associated with unstable siRNA delivery and the difficulties in delivering siRNA to the cytoplasm. If siRNA fails to disperse in the cytoplasm and is recaptured by lysosomes, SA-H_8 can once again act as a protective shield to prevent siRNA from being destroyed.

Following the successful resolution of the issue pertaining to the inadequate stability of siRNA transportation in both the body and cells, our objective is to enhance the cellular absorption and functionality of lipid nanocarriers. Consequently, our research has been centered on the utilization of cell-penetrating peptides (CPPs). Previous studies have demonstrated that CPPs exhibit the ability to bind to extracellular receptors and undergo cellular absorption, while also offering notable advantages such as strong affinity, minimal immunogenicity, and facile manufacturing [19,20]. However, it has been observed that linear CPPs exhibit a deficiency in stability and specificity [21]. Over the course of the past two decades, researchers have progressively directed their attention towards the advancement of cyclic CPPs as a means to tackle this matter [22–25]. Cyclic CPP not only encompasses the benefits of linear CPP, but also exhibits enhanced stability and heightened cell permeability [26–28]. Weerakkody *et al.* [29] has successfully synthesized a series of cyclic peptides, among which the asymmetric peptide (E_4W_5C) (Trp-Trp-Trp-Glu-Glu-Glu-Glu-Cys) exhibited superior pH-dependent performance. This peptide consists of negatively charged glucose residues on one side of the cycle and hydrodynamic tryptophan residues on the other side, thereby enhancing its potential for drug delivery applications. However, the modification of this cyclic peptide is challenging due to its significant steric hindrance. To address this limitation, we have devised a novel approach by inserting alanine residues on both sides of the cysteine, *i.e.*, (E_4W_5ACA) to provide space for the modification of the cyclic peptide. This design exhibits pH responsiveness towards cells and also enhances the intracellular drug delivery, thereby enhancing the efficiency of nanomedicine delivery [30].

To better verify the drug delivery effect of this particular design, we opted for breast cancer as the treatment model. Research has shown that Polo-like kinase 1 (PLK-1) plays a critical regulatory role in cell cycle progression [31–33]. Silencing the expression of PLK-1 using siRNA has been proven to cause cancer cell cycle arrest and apoptosis [18], while exhibiting no detrimental effects on normal cells and demonstrating favorable safety profiles. Unfortunately, the utilization of a single drug therapy that focuses on a particular pathway frequently results in inadequate effectiveness of tumor therapy and can induce the activation of compensatory pathways in cancer cells, leading to severe adverse reactions and drug resistance. Consequently, the implementation of two or more combination therapies that involve distinct mechanisms of action is anticipated to achieve higher efficacy in cancer treatment [34]. The downregulation of *PLK-1* gene expression through siRNA can enhance the sensitivity of tumor drugs to chemotherapy [35], providing potential application prospects for the combination of nucleic acid drugs and chemotherapy drugs.

In summary, this study developed a new lipid nano platform (Scheme 1), Cyclic peptide modified liposomal delivery system (Cyc-L), co-encapsulating siRNA (siPLK-1) and docetaxel (DTX) (Cyc-L_H/si-DTX) to overcome the defects of siRNA delivery. The main considerations for adopting this design are as follows: On the one hand, the combination of dioleoyl phosphatidylethanolamine (DOPE) and cholesteryl hemisuccinate (CHEMS) has better loading capacity and can contain chemical drugs and nucleic acid drugs at the same time [36,37]. On the other hand, the use of SA-H_8 to

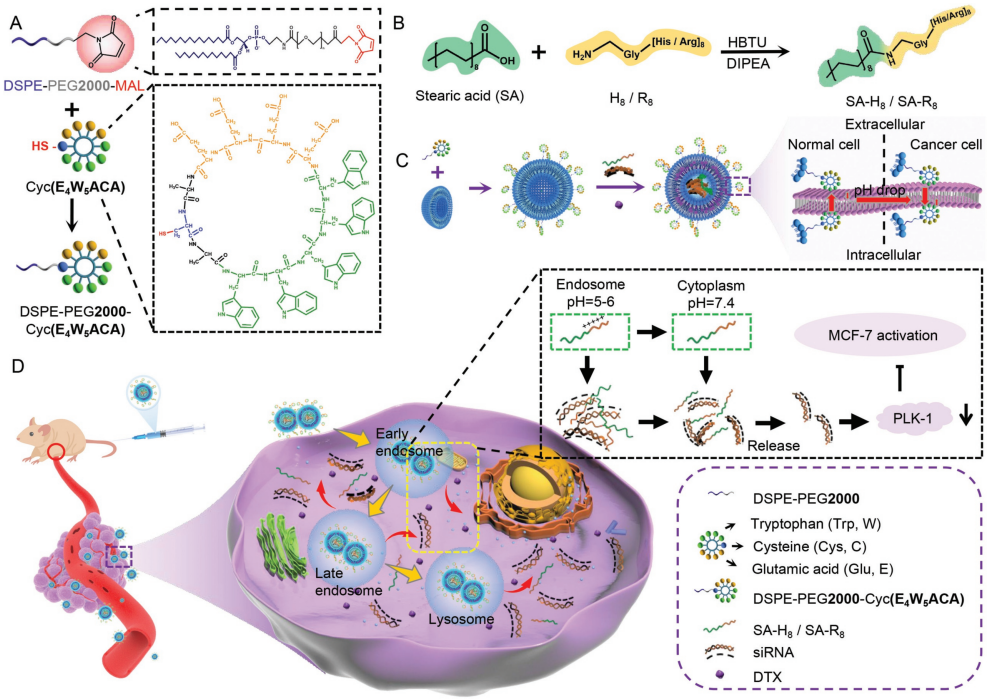

Scheme 1. Cyclic peptides modified pH-responsive co-loaded lipid nanoplatform. (A) The structure of DSPE-PEG2000-MAL and Cyc(E_4W_5ACA). (B) The prepared complexes of SA-H_8 and SA-R_8. (C) Preparation of cyclic peptides modified pH-responsive co-loaded lipid nanoplatform. (D) The processes of cyclic peptides modified pH-responsive co-loaded lipid nanoplatform *in vivo*.

compress siRNA increases the stability of siRNA and can reduce drug failure caused by drug leakage during delivery. The structure of Cyc-L_H/si-DTX allows drug delivery at different pH levels. Firstly, the addition of the outer cyclic CPP increases cellular uptake in response to pH changes. Once inside the cell, the peptide can sense the decreased pH in the endosome, aiding the liposomal drug in escaping the endosomal/lysosomal environment. When the drug reaches the cytosol, SA-H_8 responds to the higher pH, leading to the efficient release of siRNA from its complexed form. Finally, the concurrent release of siRNA and DTX in the cytoplasm demonstrates a synergistic antitumor effect. Meanwhile, the downregulation of PLK-1 by siRNA also increases the sensitivity of tumor cells to chemical drugs, which can significantly enhance the antitumor effect, reaching the effect of $1+1>2$.

The main functional material required for the multi-stage pH-responsive lipid nano platform designed in this project is DSPE-PEG2000-Cyc(E_4W_5ACA). Its synthesis route was illustrated in Fig. S1A (Supporting information), primarily involving the reaction between the thiol group on the cyclic peptide and the maleimide group. The structural formula of Cyc(E_4W_5ACA) is shown in Fig. S1B (Supporting information), comprising four main components. Firstly, four glutamic acids provide negative charges in physiological conditions, ensuring resistance to capture in the physiological environment. Secondly, five tryptophans in the structure can respond to the tumor microenvironment, enhancing the tumor's uptake of the carrier. The third part consists of cysteines, which provide active groups for the modification of functional lipid materials. To reduce steric hindrance, two alanines are added to both ends of cysteine. This design ensures the penetration effect of the cyclic peptide at the tumor site and guarantees the feasibility of functional modification. Fig. S1C (Supporting information) shows the mass spectrum of DSPE-PEG2000-Cyc(E_4W_5ACA), with the peak centered at *m/z* 4616.45 consistent with DSPE-PEG2000-Cyc's calculated mean molecule weight. This result confirmed the successful preparation of the product.

To demonstrate the pH-responsive nature, siRNA stability, and enhanced cellular uptake conferred by the cyclic peptide liposomes, we employed flow cytometry to investigate their effects on MCF-7 and A549 cells (Fig. 1). As shown in Figs. 1D and E, FAM-si (fluorescein amidite labelled siRNA) exhibited low fluorescence intensity, indicating poor stability of free siRNA and its limited ability to enter cells for sustained gene silencing effects. In contrast, N-L/FAM-si (N-L containing FAM-si) and Cyc-L/FAM-si (Cyc-L containing FAM-si) displayed significantly increased fluorescence intensity, highlighting the stabilizing effect of liposomes on siRNA. Notably, N-L/FAM-si showed no significant changes in fluorescence under different pH conditions, but Cyc-L/FAM-si demonstrated a significant increase in fluorescence intensity under acidic pH condition, indicating the excellent pH-responsive nature of Cyc and its ability to enhance drug delivery efficiency across cell membrane.

To rule out the possibility of the drug adhering to the cell membrane, leading to false-positive flow cytometry results, we further employed confocal laser-scanning microscopy (CLSM) to observe the changes in siRNA intensity in the cytoplasm of different groups. As shown in Figs. 1F and G, after several hours of incubation, FAM-si displayed minimal fluorescence intensity, while N-L/FAM-si and Cyc-L/FAM-si exhibited noticeable fluorescence. Additionally, N-L/FAM-si showed no significant fluorescence changes under different pH conditions, and Cyc-L/FAM-si exhibited a significant increase in fluorescence intensity under lower pH conditions, consistent with the flow cytometry results. Importantly, the observed fluorescence intensity of FAM-si was primarily within the cytoplasm, eliminating the possibility of false-positive results due to drug adhesion on the cell surface, which indicates the change of Cyc peptide under acidic conditions, thus mediating the translocation of liposomal siRNA across the cell membrane.

Once drugs enter the cytoplasm, they are prone to be sequestered by lysosomes, rendering them ineffective. To facilitate successful escape from lysosomes, we synthesized SA-H_8 and SA-R_8 as depicted in Fig. S2 (Supporting information), we selected SA-H_8 for siRNA compression to enhance its stability. By screening the ratio of SA-H_8 to siRNA, we ensured complete compression of siRNA by SA-H_8, as shown in Fig. 1A, The interaction of SA-H_8/phosphate with siRNA (N/P ratio) was examined using an agarose gel electrophoresis (AGE) assay. siRNA was completely compressed into the complex with an N/P ratio of 5:1. As shown in Figs. 1B and C, the liposomes were approximately spherical and had a diameter of approximately 150–200 nm, the results demonstrated that the particle size of liposomes was uniform. Subsequently, the liposomes were examined using a Malvern particle size analyzer. The particle size potential diagram is shown in Fig. S1D (Supporting information). The particle size of N-L_R/si (Non-modified lipsosome-encapsulate SA-R_8/si) was around 170 nm. The modified particle size increased slightly, but the polydispersity index (PDI) was below 0.2, indicating that the particle size was relatively uniform. As shown in Fig. S1E (Supporting information), the zeta potential results showed that the liposomes carrying siRNA on the surface were negatively charged as a whole and were relatively stable. Moreover, the liposomes showed good storage stability in phosphate buffer solution (PBS) with different pH (Fig. S1F in Supporting information). Subsequently, we prepared SA-H_8/si using this ratio to validate the enhanced lysosomal escape and prolonged gene silencing effect of compressed siRNA. We conducted experiments using MCF-7 and A549 cells under pH 6.5 conditions. As depicted in Figs. 1H and I, there was no significant difference in fluorescence intensity between SA-R_8/si and SA-H_8/si after 2 h. However, after 6 h, the fluorescence intensity of SA-H_8/si was notably stronger, indicating that siRNA compressed by SA-H_8 was more prone to escape from lysosomes, resulting in a more pronounced and lasting effect.

In the previous phase of our research, we demonstrated that the efficacy of SA-H_8/si surpassed that of SA-R_8/si (siRNA complexes compressed by SA-R_8). However, alterations in the cyclic peptide may influence the drug's behavior *in vivo*. To identify the optimal formulation, we employed the same preparation method to produce SA-R_8/si as a control. Both formulations were incubated on MCF-7 cells for 1 h and 3.5 h. As depicted in Fig. 1J, surprisingly, Cyc-L_H/FAM-si exhibited stronger and scattered fluorescence at 3.5 h, indicating that SA-H_8/si effectively facilitated the intercellular release of siRNA. Importantly, through these improvements, our multistage pH-responsive liposomal nano-system, designed with the cyclic peptide, shortened the drug uptake time within cells. This advancement represents a further enhancement of our initial design and provides favorable evidence for the subsequent design of nucleic acid drug carriers.

The aforementioned experiments validated the successful cytoplasmic release of siRNA with this design but did not confirm its therapeutic efficacy. Considering that PLK-1 knockdown induces apoptosis, to verify the therapeutic effect of this design strategy on tumors, we tested the apoptosis induction by different formulations on tumor cells using flow cytometry, as shown in Fig. 2A. Free siRNA exhibited minimal cytotoxicity to the cells, mainly due to the instability of siRNA, which is prone to enzymatic degradation in serum. The N-L/si (non-modified lipsosome-encapsulated siRNA) induced approximately 7% apoptosis cells under different pH conditions, indicating that liposomes can enhance the stability of siRNA. Moreover, the Cyc-L/si (Cyc-modified lipsosome-encapsulated siRNA) increased the cytotoxic effect on cells under different pH conditions, with a stronger impact observed in acidic conditions. In the physiological environment, although Cyc did not undergo charge reversal to increase the permeability of liposomes to cells, its rigid structure inherently en-

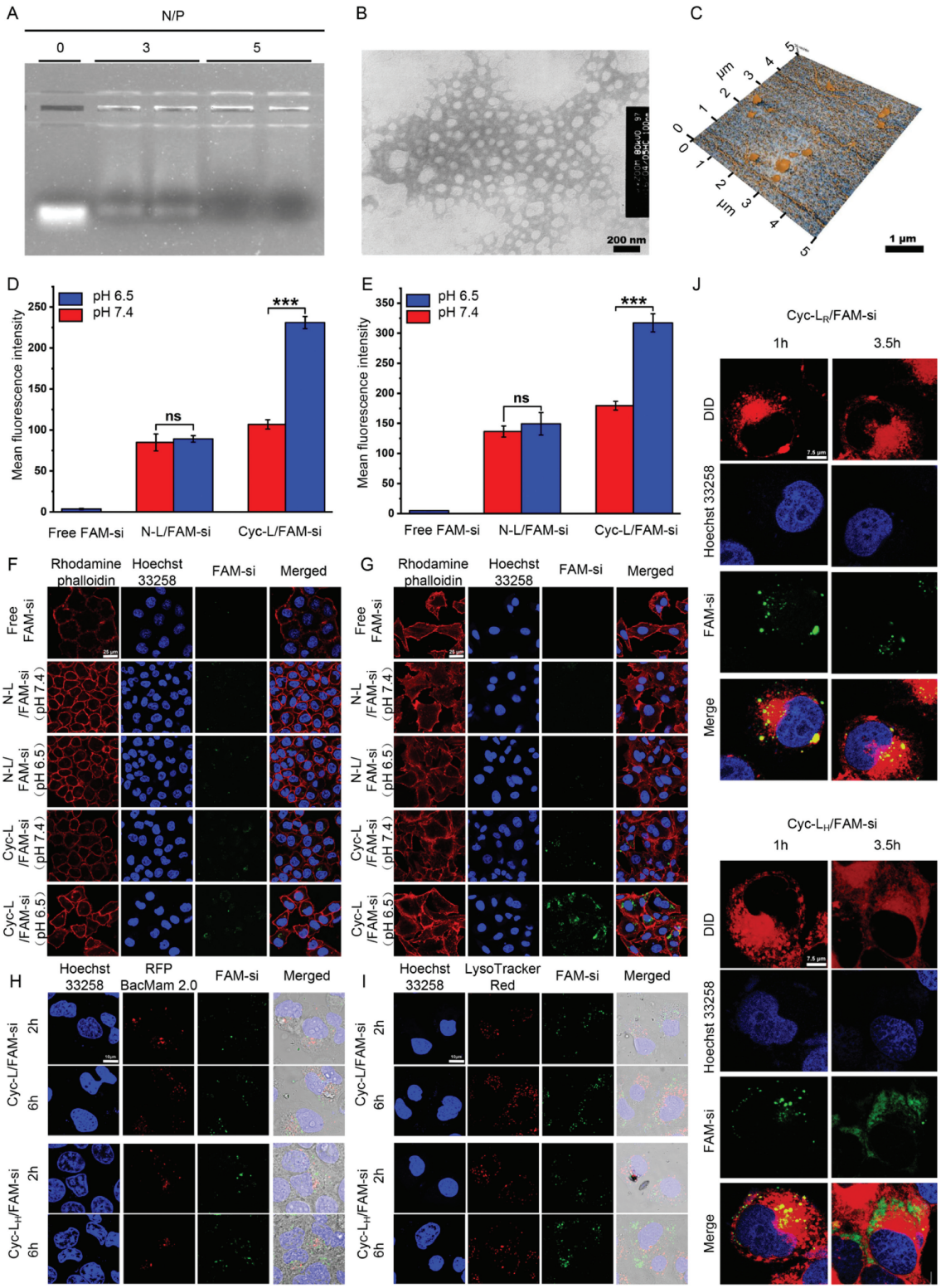

Fig. 1. Morphological characterization and intracellular trafficking of lipsomes. (A) Binding of SA-H_8 to siRNA at different N/P ratios. (B) Transmission electron microscope (TEM) characterization of Cyc-L. Scale bar: 200 nm. (C) Atomic force microscope (AFM) topographic image characterization of Cyc-L. Scale bar: 1 μm. (D) Flow cytometry was used to detect different groups of preparations uptaken by MCF-7 and (E) A549 cells ($n = 3$). Data are presented as the means ± SD. $^{***}P < 0.001$. ns, no significance. (F) CLSM was used to detect different groups of preparations uptaken by MCF-7 and (G) A549 cells. Scale bar: 25 μm. (H) FAM-si traffics intracellularly and colocalizes with early endosomes in MCF-7 cells and (I) late endosome/lysosome in A549. Scale bar: 10 μm. (J) Double-labeled liposomes were added to MCF-7 cells for 1 and 3.5 h to determine their intracellular uptake. Scale bar: 7.5 μm.

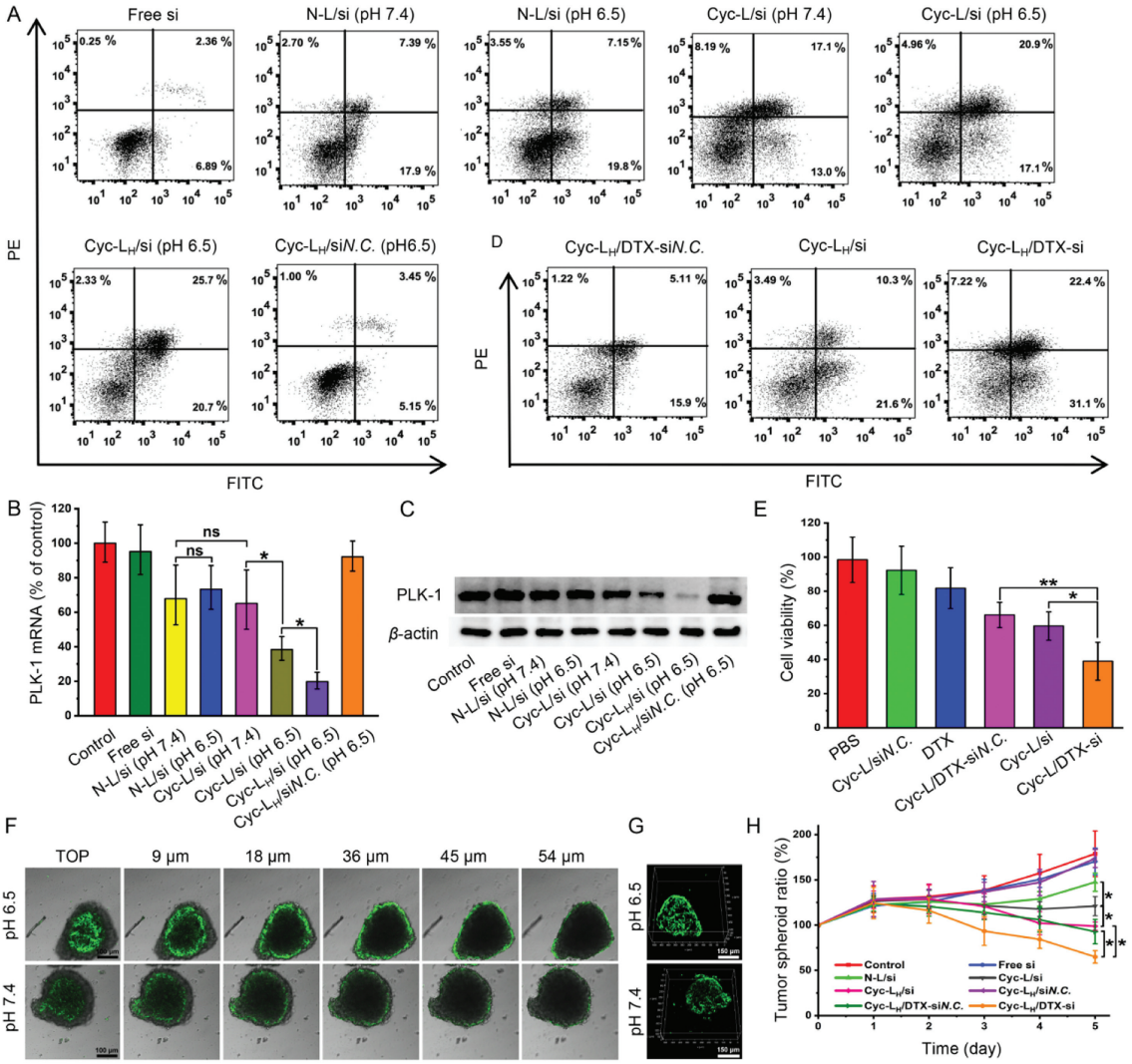

Fig. 2. Evaluating gene silencing's effectiveness and cytotoxicity. (A) Drug-loaded liposomes induce cell apoptosis. (B) qRT-PCR was used to determine the expression of PLK-1 mRNA ($n = 3$). (C) Western blot analysis was used to determine the expression of PLK-1. (D) Codelivery liposomes induce cell apoptosis. (E) Various formulations have been analyzed for their cytotoxicity ($n = 3$). (F) Images taken with confocal microscope of 3D tumor spheroids of MCF-7 cells after 24 h incubation with Cyc-L at pH 6.5 and 7.4. Scale bar: 100 μm. (G) Layer-by-layer reconstruction in 3D. Scale bar: 150 μm. (H) Ratio of tumor spheroid volume ($n = 6$). Data are presented as the means ± SD. $^{*}P < 0.05$, $^{**}P < 0.01$. PE, phycoerythrin; FITC, fluorescein isothiocyanate.

hanced the permeability of liposomes to the cell membrane, resulting in a good therapeutic effect. Furthermore, we found that Cyc-L_H/si (Cyc-modified lipsosome-encapsulated SA-H_8/si) further increased tumor apoptosis, which was within the expected range. This is mainly because SA-H_8 can protect siRNA during lysosomal escape. Once SA-H_8/si escapes into the cytoplasm, the pH change causes SA-H_8/si to disintegrate, releasing siRNA to exert its function. Therefore, Cyc-L_H/si demonstrated the optimal therapeutic effect.

Subsequently, we further investigated the rationality of this formulation design at the genetic and protein levels. As shown in Fig. 2B, we observed a significant decrease in PLK-1 mRNA levels with Cyc-L_H/si at pH 6.5 compared to pH 7.4, indicating improved siPLK-1 internalization and escape from endosomes/lysosomes. In order to determine whether the reduction in PLK-1 mRNA levels corresponds to a decrease in PLK-1 protein levels, we performed western blot analyses on MCF-7 cells. In Fig. 2C, siPLK-1 delivered *via* liposomes exclusively reduced PLK-1 expression. However, both free siPLK-1 and Negative Control-siRNA (si*N.C.*)-loaded Cyc-L_H (Cyc-L_H/si*N.C.*) had little effect on reducing PLK-1 protein levels, the results indicated that siRNAs with no definite role cannot play a role when they reach the target cells, and siRNAs with definite efficacy lack delivery vectors are prone to fail and cannot function during delivery [5]. PLK-1 protein expression was significantly inhibited only in MCF-7 cells treated with siPLK-1-loaded Cyc-L at pH 6.5, but not at pH 7.4. In addition, the lowest levels of PLK-1 protein expression were detected in cells treated with Cyc-L_H/si, providing further evidence for the anticipated pH responsivity of Cyc-L and SA-H_8 to the extracellular and intracellular tumor microenvironments, respectively.

MCF-7 cells were incubated with formulations encapsulating siPLK-1 and DTX to study the pro-apoptotic effects of their co-administered groups. As shown in Fig. 2D, transfection with Cyc-L_H/DTX-siPLK-1 (Cyc-L_H/DTX-si) resulted in an increased percentage of apoptotic cells (~53%), much higher than that of the Cyc-L/DTX and Cyc-L/DTX-si*N.C.*, which closely correlated with the results of the cell proliferation assay (Fig. 2E), demonstrating the combined inhibitory effect on cancer cells by simultaneous delivery of siPLK-1 and DTX. As a microtubule stabilizer, DTX selectively prompts cell cycle arrest in the G2/M phase, leading to subsequent apoptosis. Additionally, the suppression of PLK-1 expression halted tumor growth and heightened the sensitivity of MCF-7 cells to tax-

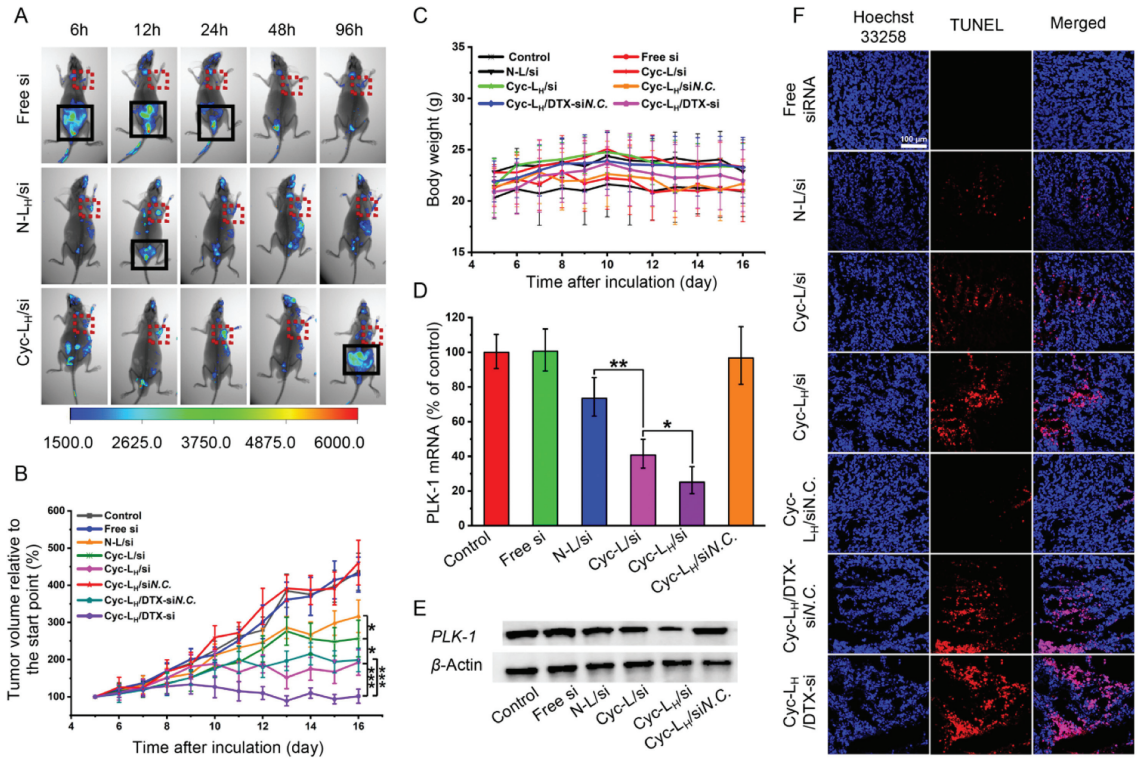

Fig. 3. The antitumor activity of different formulations *in vivo*. (A) A fluorescent imaging study of tumor-bearing nude mice given Cy5-siRNA formulations *in vivo*. (B) An analysis of the changes in tumor volume and (C) body weight in MCF-7 tumor-bearing mice treated with different formulations ($n = 6$–7). (D) Detection of mRNA and (E) protein in tumors 24 h after last administration ($n = 3$). (F) Slices of MCF-7 tumor stained with TUNEL. Scale bar: 100 μm. Data are presented as the means ± SD. $^{*}P < 0.05$, $^{**}P < 0.01$, $^{***}P < 0.001$.

ane treatment. Consequently, the simultaneous delivery of siPLK-1 and DTX halts the cell cycle progression and subsequently enhances the occurrence of apoptosis.

While significant therapeutic efficacy was achieved in the above results, the validation was limited to a two-dimensional cellular context. The elevated interstitial fluid pressure (IFP) at tumor sites significantly hampers the permeability of drug delivery systems, limiting their therapeutic applications [38]. Three-dimensional tumor spheroids, which mimic the solid tumor's pathological environment, including interstitial pressure and cellular network, serve as a bridging model between two-dimensional cells and animal models [39]. MCF-7 tumor spheroids were utilized to evaluate Cyc-L/si penetration at different pH values (pH 6.5 and 7.4) using CLSM. In Figs. 2F and G, a stronger fluorescence signal was observed in the core spheroids after treatment at pH 6.5, these results indicated that the preparation was able to increase the penetration of the drug under acidic conditions, further indicating the cell penetration ability of Cyc peptide.

The control group in Fig. 2H showed that PBS (pH 6.5) treatment led to a 1.8-fold increase in the average spheroid volume after 5 days, indicating the rapid growth of the cancer. Free siRNA and Cyc-L_H/si*N.C.* had minimal inhibitory effects. However, Cyc-L/si exhibited significantly enhanced antitumor effects ($P < 0.05$) compared to N-L/si. Furthermore, when combined with SA-H_8 compressed siPLK-1, Cyc-L_H/si further enhanced inhibitory effects on the growth of tumor spheroids, reducing the spheroid volume to 96% of the initial value after 5 days. These results support that the combined effect of Cyc and SA-H_8 enhances the inhibitory effect on tumor spheroid growth. Furthermore, Cyc-L_H/DTX-si had a remarkable inhibitory effect on the growth of MCF-7 tumor spheroids, this is supposed to be attributed to the combined chemotherapeutic DTX and gene therapeutic siPLK-1delivery system.

In vivo, imaging experiments investigated the biodistribution of siRNA-loaded liposomal systems in MCF-7 tumor-bearing mice. All procedures involving animal housing and treatment were approved by the Institutional Authority for Laboratory Animal Care of Hebei Medical University. Cy5-labeled N-L_H/si and Cyc-L_H/si were administered to MCF-7 xenograft tumor models, respectively, and tissue distribution was recorded, in which the red dotted box was the tumor inoculation location and the black solid box was the metabolic excretion location of mice. As shown in Fig. 3A, we can see that free-si began to be metabolized at 6 h, and only a small amount of fluorescence accumulated at the tumor site, and no fluorescence accumulated at the tumor site after 12 h, mainly because the siRNA was not stable *in vivo* and was easily degraded by enzymes *in vivo*. After 6 h of tail i.v. injection, there was an obvious accumulation of fluorescence at the tumor site, and no obvious metabolism was observed, and after 12 h, we could observe a large amount of accumulation of fluorescence at the excretion site, but most of it had been excreted, indicating that the excretion time of the N-L_H/si group was 6–12 h, the fluorescence accumulated the most at the tumor site at 12 h, and the accumulation of fluorescence at the tumor site could still be observed until 48 h, which showed that the liposomes could prolong the circulation time of siRNA *in vivo*, while the Cyc-modified liposomes were only observed to be metabolized from the body at 96 h, and strong fluorescence could still be observed in the axillary of mice at 96 h, indicating that the Cyc-modified liposomes could not only prolong the circulation time of the drug *in vivo* but also had good tumor permeability.

We measured the size of the tumor volume of nude mice after treatment (i.v. injection), and the results were shown in Fig. 3B, which confirmed that Cyc-L_H/DTX-si has the best treatment effect, mainly because the modification of Cyc provides better drug retention and penetration in the tumor site, and the synergistic administration of DTX and siRNA improves the treatment effect, while

the use of siRNA alone has no treatment effect compared with the control group treated with 5% glucose, which once again verifies the instability of siRNA. Compared with Cyc-L/si, N-L/si only had a slight inhibitory effect on tumor growth, while the Cyc modification group significantly inhibited the tumor growth rate ($P < 0.05$), indicating that Cyc modification enhanced liposomal siPLK-1 antitumor effect *in vivo*. Furthermore, in order to verify the contribution of SA-H_8 to siRNA, we investigated the inhibitory effect of Cyc-L_H/si compared with Cyc-L/si on tumors, and the results were consistent with cell experiments and SA-H_8 could significantly improve the effect of siRNA on tumors. In order to rule out the effect of Cyc-L_H on tumors, we encapsulated Cyc-L_H with si*N.C.*, which showed no therapeutic effect compared with the control group, which showed that the Cyc-L_H/DTX-si experimental design was reasonable and the results were reliable.

In this study, we assessed the antitumor efficacy of Cyc-modified liposomes co-loaded with DTX and siPLK-1 using an MCF-7 xenograft model. Cyc-L_H/DTX-si significantly inhibited tumor growth, resulting in a much smaller tumor size compared to the DTX and siRNA group ($P < 0.001$). These findings highlight the potent antitumor effects of Cyc-L_H/DTX-si, mainly because PLK-1 and DTX work together, PLK-1 can kill tumor cells on the one hand, and increase the sensitivity of chemical drugs to tumor cells on the other hand, so that it can exert a greater effect (Fig. 3C), we found no significant change in the body weight of mice in the treatment group compared to the control group. These results suggest that there was no significant difference between the liposomes group and the control group, indicating negligible acute or severe toxicity associated with the tested dose of the treatment.

To investigate the correlation between the observed tumor growth inhibition and *PLK-1* gene silencing, we conducted a comprehensive analysis of PLK-1 expression at both the mRNA and protein levels in tumor tissues. This was achieved through quantificational real-time polymerase chain reaction (qRT-PCR) and Western blot analyses. As depicted in Figs. 3D and E, the mRNA and PLK-1 protein expressions in the free siRNA group or the Cyc-L/si*N.C.* group were comparable to those in the 5% glucose group. In contrast, the liposome groups loaded with siPLK (N-L/si, Cyc-L/si, and Cyc-L_H/si), especially Cyc-L_H/si, exhibited a significant reduction in both mRNAs and protein levels. Notably, the addition of SA-H_8 in the Cyc-L_H/si group induced a more pronounced silencing of the *PLK-1* gene. These findings align with the previously observed antitumor effects, establishing a direct and consistent link between the retardation of tumor growth and *PLK-1* gene silencing.

The assessment of tumor cell apoptosis was conducted through terminal deoxynucleotidyl transferase (TdT)-mediated dUTP nick end labeling (TUNEL) following the study treatment, as illustrated in Fig. 3F. In the control group, which included free siPLK-1 and Cyc-L_H/si*N.C.*, no TUNEL-positive tumor cells (depicted in red) were detectable, indicating no apparent apoptosis. Conversely, the TUNEL assay revealed an increased level of apoptosis when using Cyclic peptide modified nanosystem compared to non-mondifed one, and coloading group compared to the siRNA or DTX one.

In this research, a cyclic pH-responsive peptide was engineered to effectively target the highly acidic microenvironment within tumors. Various environmentally responsive lipid delivery systems have been developed due to the unique characteristics of the tumor microenvironment, particularly pH changes at the tumor site. However, these systems mostly respond to a single pH change, such as enhancing effective cellular uptake or selective drug release. They seldom adjust to the entire process encountered by the drug. A pioneering multi-level pH-responsive liposomal system was constructed for the simultaneous delivery of Cyc-L_H/DTX-si. Additionally, SA-H_8 was employed to condense siRNAs, facilitating efficient release into the cytoplasm. The Cyc-modulated liposomal system exhibited substantially heightened cellular uptake, favorable evasion from endosomes/lysosomes, and effective diffusion of payload into the cytoplasm. As a consequence of this co-delivery system, the *PLK-1* gene was significantly silenced, MCF-7 cells were induced to apoptotic, and tumor spheroids were impermeable and inhibited. Specifically, the Cyc-L_H/DTX-si co-delivery system displayed the most significant impact by impeding cell proliferation, curtailing tumor spheroid growth, and constraining tumor expansion *in vivo*. Given its adept intratumor penetration, cytoplasmic release mechanism, and remarkable therapeutic efficacy for both lipophilic therapeutic agents (DTX) and nucleic acid-based active biomolecules (siRNA), this Cyc-mediated pH-responsive platform exhibits substantial promise for amalgamated chemo/gene therapy.

Declaration of competing interest

The authors declare that they have no known competing financial interests or personal relationships that could have appeared to influence the work reported in this paper.

Acknowledgments

This work was supported by the grants from the National Natural Science Foundation of China (Nos. 81973251 and 81302725), Hebei Province Funding Project for Introduced Overseas Personnel (Nos. C20230351 and C20220345), Key Research and Development Program of Hebei Province (No. 22372701D), Hebei Province Natural Science Fund (No. H2020206610), Hebei Provincial Health Commission Government-Funded Clinical Medicine Talent Program (No. ZF2024048), and Hebei Medical University Undergraduate Innovative Experiment Program (No. USIP2023008).

Supplementary materials

Supplementary material associated with this article can be found, in the online version, at doi:10.1016/j.cclet.2024.109660.

References

[1] A.M. Mallick, A. Biswas, S. Mishra, et al., Chem. Sci. 14 (2023) 7842–7866.
[2] T.C. Roberts, R. Langer, M.J.A. Wood, Nat. Rev. Drug Discov. 19 (2020) 673–694.
[3] Y. Guo, X. Cao, X. Zheng, et al., Natl. Sci. Rev. 9 (2022) nwac006.
[4] K. Yadav, K.K. Sahu, Sucheta, et al., Int. J. Biol. Macromol. 241 (2023) 124582.
[5] R. Kumar, C.F. Santa Chalarca, M.R. Bockman, et al., Chem. Rev. 121 (2021) 11527–11652.
[6] K. Tatiparti, S. Sau, S.K. Kashaw, A.K. Iyer, Nanomaterials 7 (2017) 77.
[7] A.K. Abosalha, J. Boyajian, W. Ahmad, et al., Expert Rev. Clin. Pharmacol. 15 (2022) 1327–1341.
[8] S. Khan, U. Rehman, N. Parveen, et al., Expert Opin. Drug Deliv. 20 (2023) 1167–1187.
[9] M. Friedrich, A. Aigner, BioDrugs 36 (2022) 549–571.
[10] B. Hu, L. Zhong, Y. Weng, et al., Signal Transduct. Target. Ther. 5 (2020) 101.
[11] S. Guo, M. Zhang, Y. Huang, Trends Mol. Med. 30 (2024) 13–24.
[12] H. Hedlund, H. Du Rietz, J.M. Johansson, et al., Nat. Commun. 14 (2023) 1075.
[13] Y. Yan, G. Zhang, C. Wu, et al., ACS Biomater. Sci. Eng. 8 (2022) 1964–1974.
[14] S.S. Ali Zaidi, F. Fatima, S.A. Ali Zaidi, et al., J. Nanobiotechnol. 21 (2023) 381.
[15] Y. Liu, L. Huang, Methods Mol. Biol. 2282 (2021) 159–169.
[16] P.E. Saw, X. Xu, M. Zhang, et al., Angew. Chem. Int. Ed. 59 (2020) 6249–6252.
[17] W. Zhang, Y. Jiang, Y. He, et al., Acta Pharm. Sin. B 13 (2023) 4105–4126.
[18] T. Zhao, C. Liang, Y. Zhao, et al., J. Nanobiotechnol. 20 (2022) 177.
[19] F. Guo, Q. Fu, K. Zhou, et al., J. Nanobiotechnol. 18 (2020) 48.
[20] S. Yu, H. Yang, T. Li, et al., Nat. Commun. 12 (2021) 5131.
[21] K. Kardani, A. Milani, H.S.S.A. Bolhassani, Expert Opin. Drug Deliv. 16 (2019) 1227–1258.
[22] H. Zhang, S. Chen, RSC Chem. Biol. 3 (2022) 18–31.
[23] P.G. Dougherty, A. Sahni, D. Pei, Chem. Rev. 119 (2019) 10241–10287.
[24] L.K. Buckton, M.N. Rahimi, S.R. McAlpine, Chemistry 27 (2021) 1487–1513.
[25] D. Feng, L. Liu, Y. Shi, et al., Chin. Chem. Lett. 34 (2023) 108026.
[26] N.A. Abrigo, K.K. Dods, C.A. Makovsky, et al., ACS Chem. Biol. 18 (2023) 746–755.
[27] L. Ling, A.S. Raikhel, Proc. Natl. Acad. Sci. U. S. A. 118 (2021) e2023470118.
[28] S. He, Y. Fang, M. Wu, et al., J. Med. Chem. 66 (2023) 16828–16842.
[29] D. Weerakkody, A. Moshnikova, N.S. El-Sayed, et al., Sci. Rep. 6 (2016) 31322.
[30] J. Zhang, Y.X. Cui, X.N. Feng, et al., ACS Appl. Mater. Interfaces 11 (2019) 39624–39632.
[31] D.S. Benoit, S.M. Henry, A.D. Shubin, et al., Mol. Pharm. 7 (2010) 442–455.

[32] C.E. Cunningham, M.J. MacAuley, F.S. Vizeacoumar, et al., Cancers 12 (2020) 2953.
[33] G. Kara, G.A. Calin, B. Ozpolat, Adv. Drug Deliv. Rev. 182 (2022) 114113.
[34] M. Zeinali, S. Abbaspour-Ravasjani, M. Ghorbani, et al., Drug Discov. Today 25 (2020) 1416–1430.
[35] J. Zhang, L. Zhang, J. Wang, et al., J. Med. Chem. 65 (2022) 10133–10160.
[36] J. Karlsson, Y. Rui, K.L. Kozielski, et al., Nanoscale 11 (2019) 20045–20057.
[37] J. Karlsson, K.R. Rhodes, J.J. Green, S.Y. Tzeng, Expert Opin. Drug Deliv. 17 (2020) 1395–1410.
[38] A.L.B. Seynhaeve, M. Amin, D. Haemmerich, et al., Adv. Drug Deliv. Rev. 163-164 (2020) 125–144.
[39] Q. Guo, X. He, C. Li, et al., Adv. Sci. 6 (2019) 1901430.